Eur. Phys. J. B (2018) 91: 321
https://doi.org/10.1140/epjb/e2018-90540-7

THE EUROPEAN PHYSICAL JOURNAL B

Regular Article

Good influence transmission structure strengthens cooperation in prisoner's dilemma games

Penghui Liu and Jing Liu[a]

Key Laboratory of Intelligent Perception and Image Understanding of Ministry of Education, Xidian University, Xi'an 710071, P.R. China

Received 11 September 2018 / Received in final form 30 September 2018
Published online 21 December 2018

Abstract. Analysis on how network reciprocity may help promote the coordination of agents in a system has attracted attention. However, designing effective methods for searching highly cooperative population structures remains a challenge. In this article, we reveal how cooperation behavior survives and spreads from a micro perspective, and further visualize the topology of influence transmission structure that supports the spread of cooperation. Based on our analysis, a highly cooperative multilevel scale-free network (mlSFNs) model is designed and compared with other existing scale-free network models. Meanwhile, we discover the positive correlation between influence coverage rate and cooperation level from a correlation analysis toward mass sample data. Thus, we introduce one rule for highly cooperative structures: influence coverage rate is essential to cooperation, while the unaffected nodes should be less influential. In our experiments, we find that this rule can provide effective guidance to the structure optimization algorithm termed fMA-C_{PD}-SFN, which successfully optimizes various structures subject to different strategy update rules. Moreover, fMA-C_{PD}-SFN is also applicable to the optimization of large-scale populations. In this case, we conclude that this rule is instructive for future design of a highly cooperative population structure.

1 Introduction

Many problems in the reality can be represented by networked systems. With the rapid growth of technology, the demand to design and regulate a network system has been a common challenge, especially when the scale of system is large. Even if artificial intelligent has achieved great progress, researchers find it is still hard to extend existing single-agent methods to a multi-agent system [1]. Some researchers have employed the evolutionary game theory to deal with this problem, and they considered learning from the organization of real population may be significantly helpful in constructing a large-scale multi-agent systems.

Game theory has long been used to describe and analyze the interactions between self-interested individuals [2–11]. Quite a lot of attention has been paid to investigate and explain the emergence of cooperation among the rational individuals. One of the most important progresses made in this field is the network reciprocity proposed by Nowak et al. [2]. They have revealed that topology constraints influence the evolution of cooperation, have been also confirmed years later. Thereafter, many researches have contributed to the study of network reciprocity in the background of evolutionary graph theory [12–14]. Population structures were considered to be essential in the evolution of cooperation [15] and cooperators in Prisoner's Dilemma Games (PDG) forms clusters to defend against the invasion of defectors [16]. Many extended works have contributed to the correlation investigation between some network properties and cooperation. Researchers found that heterogeneity [9,17–19] promotes cooperation in social dilemma games, and hubs plays a particular role in the evolution of cooperation. However, some researchers also pointed out that the effect of hubs can be largely diminished if degree-normalized payoff value is applied [20,21]; this situation will not be considered in this article. Besides, some researchers have paid attention to analyze the importance of influence players in populations [22–24]. Considering interaction commonly exists between different life levels, researchers further focused on the evolutionary game in interdependent networks [25–30]. Recently, some researchers diverted their attention to investigate how the topology dynamics may influence the evolution dynamics. One of the most influential progresses made in the near decades is the introduction of coevolutionary rules first designed and proposed by Zimmermann et al. [31]. They considered that individuals may dynamically adjust their interaction with other players based on their gaming results [32–38]. Those works in

[a] e-mail: neouma@mail.xidian.edu.cn

this field provided us a new perspective to understand the self-reorganization of populations in nature.

Most recently, Allen et al. provided a solution for weak selection that applied to help understand the evolutionary dynamics on any population structures [39]. They reflected how small changes in population structure may influence the evolutionary outcome. Even so, no application algorithm has been designed to verify its effect on engineering issues. Thus, its significance in practically helping the optimization of a given population structure remains unknown. In our previous work [40] we successfully introduced the heuristic optimization algorithm [41–50] to reorganize a given structure. Corresponding simulation results reflected that a network structure can be reorganized and further obtain a high cooperation level, even if its degree distribution remains unchanged. Besides, some structure properties believed positive to cooperation promotion are found to fail in the actual optimization scenario, such as the clustering coefficient [51].

The difference between our work and most of the previous research is that we try to design an algorithm or a rule that may help optimize the structure of a given network and keeps its degree distribution unchanged. However, most of the preceding research focused on revealing the network properties that may contribute to coordination of system or introducing how an intrinsic mechanisms of system may push the evolution of cooperation. In contrast, our research attempts to provide guidance to how we may adjust the network system instead of relying on the self-adjustment of the system and reveal a more general rule that a cooperative structure may follow in the practical optimization process.

Different from our previous research [40] that simply searched the solution space of network structures without prior experience, in this article we attempt to introduce a more general rule that can be employed as an efficient prior experience to accelerate the optimization process. In this way, we not only obtain a method that can reduce the complexity of the optimization problem but also verify a rule's generality through a large number of successful optimization cases subject to different sizes and strategy update rule. Our work in this article can be summarized as follows. (1) We analyze the game dynamics in the spatial structure from a micro perspective and reveal how cooperation spread in heterogeneity structures. (2) We further introduce and virtualize a structure named as influence transmission structure that contributes to the cooperation based on our analysis results. Meanwhile, a network model termed multilevel scale-free networks (mlSFNs) is proposed and illustrated to be highly cooperative. (3) We discover a positive correlation between cooperation and influence structure, and further summarize a rule for the cooperative structures. (4) We employ this rule as a prior experience to optimize structures with different sizes under different strategy update rule, and found out that it can provide an efficient guidance to the optimization algorithm.

The rest of this paper is organized as follows. An overview of game dynamics on the structured populations and the definition of influence transmission structures are provided in Section 2. Details of multilevel scale-free network model are given in Section 3. Section 4 describes the details of fMA-C_{PD}-SFN and the investigation about the correlation between cooperation and influence coverage rate. Experimental results are provided in Section 5. Finally, the conclusion is provided in Section 6.

2 Prisoner's dilemma games on structured populations and influence transmission structures

In this section, we first review the prisoner's dilemma game and analyze game dynamics upon the structured population from a micro perspective. Then, based on our analysis results on how cooperation survives and spreads, we introduce the influence transmission structure to extract and visualize the topology that supports the spread of cooperation in corresponding population structure.

The prisoner's dilemma game is a useful tool to simulate the competition between organisms. In the PDG, players can select their strategies from defection ($D : s_x = 0$) and cooperation ($C : s_x = 1$). Their payoff depends on their strategy combination: The defector receives the highest payoff T if its opponent cooperates and bears the cost S. If the two players select the same strategy, they will receive R for cooperation and P for defection. In this article, we set $R = 1, P = S = 0$, and $T = 1 + r$, where r represents the advantage of defectors over cooperators.

To simulate the realistic competition and analyze the evolution of species, researchers pay attention to investigate the infinite evolutionary game dynamics that arise whenever reproductive success is influenced by interactions with others. Even if there are various strategy update rules existing in this field, the fittest is most likely to survive and reproduce.

In this article, we focus on analyzing the game dynamics under the proportional imitation and further generalize our conclusions to other strategy update rules. When a site x is updated, the current occupant and all its neighbors compete to reproduce their offspring that succeed their strategies in site x. The probability for a neighbor y to successfully reproduce is

$$W_{s_x \leftarrow s_y} = \begin{cases} (P_y - P_x)/(Dd_>), & P_y > P_x, \\ 0, & P_y < P_x, \end{cases} \quad (1)$$

where P_i and d_i respectively denotes the payoff and the degree of node i and $d_> = \max\{d_x, d_y\}$, $D = T - S$. Apparently, with probability $W_{s_x \leftarrow s_x} = \prod_l (1 - W_{s_x \leftarrow s_y})$, the focal individual reproduces and the strategy in site x remains unchanged. The relative probability for the success of neighbor y is $W_{sx \leftarrow sy} / \Sigma_l W_{sx \leftarrow sy}$, where l denotes the neighborhood of x. In this article, we employ the synchronous update method to update the whole population.

The payoff of an individual is accumulated from its interactions with all neighbors. Suppose p percent of its neighbors select to cooperate, its payoff can be estimated as

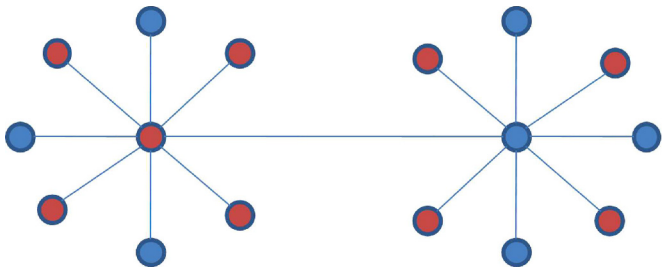

Fig. 1. A simplified game structure for analyzing the interaction between different hub nodes. We suppose the hubs do not share neighbors. Red color is employed to denote the defectors while blue color denotes the cooperators.

$$P_x = \begin{cases} pd_xR + (1-p)d_xS, & s_x = 1, \\ pd_xT + (1-p)d_xP, & s_x = 0. \end{cases} \quad (2)$$

Existing research reveals that cooperators tend to occupy the hubs of structure and spread its strategy. Therefore, we construct a simplified structure model as given in Figure 1 to analyze corresponding game dynamics from a micro perspective. Obviously, star network is a classic micro structure to help explain how cooperation in the hubs spreads. Therefore, the simplified structure is comprised of two interconnected star networks. To simplify and analyze how cooperation spreads between hubs, only centers of star networks are interconnected.

The analysis of game dynamics from the micro perspective has been studied [52]. However, we attempt to analyze how cooperation survives and spreads from a micro perspective, thereby summarizing methods that may help promote the structures of populations.

Individuals in the population are randomly initialized with strategies. Thus, if hubs (x and y) in Figure 1 are, respectively, initialized as defector and cooperator, their payoff can be obtained by equations (3) and (4). Combined with equation (1), it is obvious that only when $P_y \geq P_x \propto d_y \geq \alpha d_x$ y (cooperator) will not be slaughtered by x (defector). Here, we can obtain α by solving the inequality $P_y \geq P_x$. Meanwhile, other individuals are very likely to imitate the strategy in the hub site. Corresponding game dynamics can be illustrated in Figure 2. Obviously, the probability that y may be slaughtered decreases during the game process. Therefore, a population structure with a high cooperation level should protect cooperators from the slaughter of defectors at the initial game.

$$P_x = p(d_x - 1)T + (1-p)(d_x - 1)P + T \quad (3)$$

$$P_y = p(d_y - 1)R + (1-p)(d_y - 1)S + S. \quad (4)$$

When each node x in a graph has a neighbor that satisfies $d_y \geq \alpha d_x$ as shown in Figure 3 and the corresponding game dynamic satisfies the micro game dynamics in Figure 2, then cooperation finally dominates if the top node (n) is initialized as a cooperator.

As already mentioned, we have analyzed the situation when a cooperator will not be invaded by its defective neighbors at the initial game. Moreover, the ideal connection sequence reveals the potential widespread of cooperation if the micro game process in Figure 2 is satisfied. To intuitively illustrate and analyze such connection sequences in a population structure, we introduce the influence transmission structures that are represented by directed graphs. Neighbor y that satisfies $d_y \geq \alpha d_x$ is considered as having influence on the focal site x: directional connection from y to x exists. Corresponding influence transmission structure can be obtained as given in Figure 4.

To be mentioned, influence transmission structures intuitively describe how cooperation may survive at the current stage and further spread in the following generations. For example, if $d_y \geq \alpha d_x$ and y is initialized as cooperator, then y will not be slaughtered by imaginary defector x. On the contrary, y may spread its strategy to x in the following generation. Therefore, population structures with reasonable influence transmission structures benefits the spread of cooperation. Of particular note is that the influence transmission structure may dynamically change during the game process, because α dynamically changes with the distribution of strategy. To optimize population structure subject to random initialization of strategies, we only focus on the influence transmission structure at the initial stage when the percent of cooperative neighbors around each focal site is equal.

3 Multilevel scale-free network model

Most real networks are found to be similar to scale-free networks. Existing research reveals the positive effect of heterogeneity to the emergence of cooperation [9,17]. Thus, analyzing the cooperation on scale-free networks has become more and more important.

In the previous section, we analyzed game dynamics upon structured populations from a micro perspective and introduced the influence transmission structure to visualize our analysis results. In this section, we further combine our analysis conclusions with the design of a scale-free structure model and investigate its difference with other existing scale-free structures in terms of structures and corresponding influence transmission structures.

Albert et al. first introduced the preferential attachment and proposed the Barabási Albert networks (BANs) [53]. They assumed that individuals with larger neighborhood are more attractive to new members. However, Holme and Kim networks (HKNs) were proposed to make a balance between the global and local connections [51]. With the increasing of construction parameter p (details in Ref. [51]), a new member becomes more likely to connect with neighbors of its first connected node. Assenza et al. declaimed that cooperation level of the constructed structures climbs up with the increase in p [51]. What should be noted is that, when $p = 0$, there is no difference between HKNs and BANs.

Based on the analysis provided in the previous section, two rules can be concluded for the construction of highly cooperative network model: (1) corresponding influence transmission structures should take in nodes as many as possible and approximate the ideal structures (Fig. 3) and

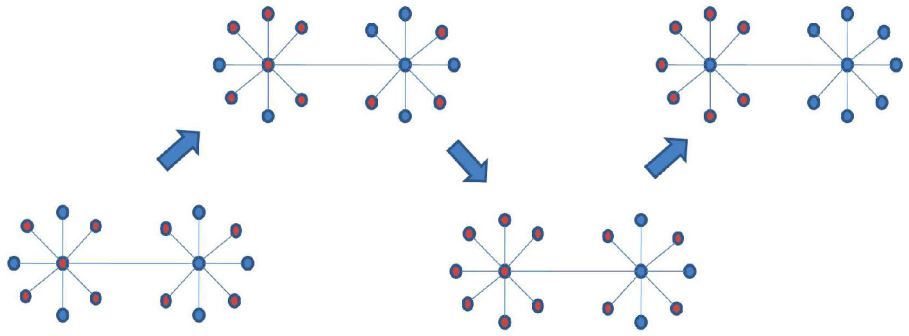

Fig. 2. Game evolution upon the simplified structure. These neighbors around hubs are likely to imitate the strategy in the hub site. Therefore, in the following generations, payoff of cooperators increases while that of defectors decreases, which leads to the rapid decrease of the probability $W_{sy} \leftarrow s_x$.

Fig. 3. The connection sequence follows $d_i \geq \alpha d_{i-1}$.

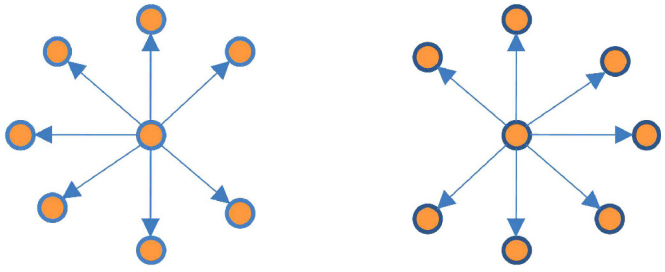

Fig. 4. The influence transmission structure of the simplified structure in Figure 2. Directed edges represent the influence direction: if x has influence upon y, x may spread cooperation to y in the following generations. Therefore, for the influence transmission structure at the initial stage, nodes with small degrees are under the influenced of the hubs. While the influence to the two hubs above is necessary, nodes with larger degrees are required.

(2) hubs should share fewer neighbors to satisfy the micro game dynamic.

Based on the above rules, in our design of scale-free structures, we pay more attention to the local heterogeneity. In the construction of HKNs, neighbors of the first connected node are selected with equal probability. However, neighbors in our design are selected according to the preferential attachment, because the local heterogeneity can effectively enhance the influence of some neighbors and thereby satisfy rule (1). To satisfy rule (2), some neighbors with the largest degree are considered as potential hubs and filtered from the selection to shrink corresponding shared neighborhood. Most importantly, in the construction of HKNs, the new member always connects with neighbors of the first selected node (reference node) if corresponding probability is satisfied. However, in our design, the corresponding reference node changes during the selection. The reference is the newest connected node with reasonable neighbors that can be further connected with. Obviously, heterogeneity in our design is enhanced from different levels: from global to local, from the newest connected node to the oldest one. Thus, this scale-free structure design is termed as multilevel scale-free network in our article. The corresponding construction method is summarized in Algorithm 1.

What should be noted is β in our experiments is set to 0.8. The comparison among BANs, HKNs, and mlSFNs in terms of their network structures and influence transmission structures is provided in Figures 5 and 6. Apparently, BANs have a closer structure while the structures of the others are more hierarchical. Meanwhile, we find that the influence transmission structures of mlSFNs are the largest after comparing their average influence coverage rate: the percent of nodes that its neighbor satisfy the condition $d_y \geq \alpha d_x$ when $r = 1$.

The cooperation level of these three network structures obtained under different r is shown in Figure 7. Apparently, mlSFNs have the highest cooperation level while HKNs ($p = 1$) follows. Meanwhile, the corresponding influence coverage rate follows the same trend. Therefore, combining with the analysis of game dynamics provided in the previous section, we preliminarily conjecture that there is a positive correlation between cooperation and influence coverage rate, which will be further verified by the following experiments.

4 Fast structure optimization algorithm for highly cooperative population structures

In the previous section, we preliminarily conjectured that there is a positive correlation between cooperation and influence coverage rate. Therefore, in this section, we further investigate this correlation and complement a rule that may be shared by cooperative structures. Finally, this rule is employed to the optimization algorithm to verify its value in optimizing structures toward higher cooperation level.

We start our correlation analysis between cooperation and influence coverage rate with a more rigorous and reliable data analysis. We use BANs, HKNs, and mlSFNs as seeds of networks to produce more general scale-free structures. However, we randomly adjust those seeds produced based on the edge switch method to effectively sample

Algorithm 1: Multilevel scale-free network

Input:
n: number of connection;
N: Scale of network;
β: Filter parameter;
m_0: Initial number of nodes;
Output:
G: Multilevel scale-free network;

1: Initialize the graph with m_0 fully connected nodes;
2: **for** $i = 1$ to N-m_0 **do**
3: $\Omega \leftarrow \emptyset$; // List of connected nodes and index indicates the connection order. (the 1st record is the first connected node)
4: A new node x is added into the graph;
5: Connect x with a node y from the current graph based on the preferential attachment;
6: $\Omega \leftarrow \Omega \cup y$; //$y$ is the 1st record
7: **for** j= 1 to $n - 1$ **do**
8: **for** the records z in Ω from kth downto 1st do //k is the number of records in the current list.
9: $\Theta \leftarrow$ Extract neighbor the degree of nodes z;
10: Sort Θ in descending order according to degree of nodes;
11: $\Theta \leftarrow$ Remove $(1- \beta)$ nodes with the largest degree from Θ;
12: **if** $\Theta \not\subset \Omega$ then
13: **break**;
14: **end**;
15: **end;**
16: connect x with a node still not connected in Θ according to the preferential attachment;
17: **end;**
18: **end.**

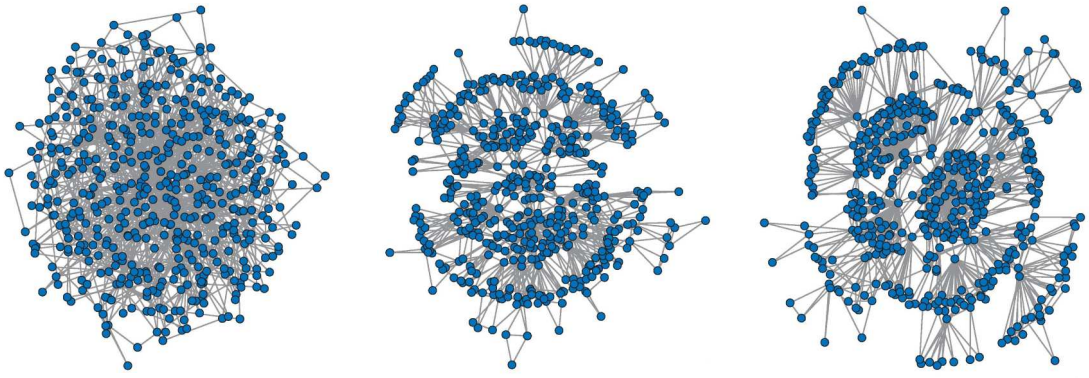

(a) (b) (c)

Fig. 5. Network structures of BAN (a), HKN: $p = 1$ (b), mlSFNs (c) while the size of networks is 500, $m_0 = 2$, and average connection $z = 4$. These graphs are drawn by Pajek under the same layout style. Apparently, BANs have closer structures, while structures of the others are more hierarchical.

the structure solution space. Meanwhile, the hill climbing method is combined to control sampling direction in terms of structures' influence coverage rate. This is designed to help fully explore the relational data space. As the adjustment is a completely random operation, the hill climbing method will not influence the true pattern of relational data.

To control the density of samples and expend the sampling space, different adjustment scales are employed in our experiments. That means a given structure will be adjusted by the edge switch method for s rounds before it is evaluated. Details of the sampling methods are summarized in Algorithm 2 and the edge switch method is provided in Figure 8. The corresponding parameters of the sampling methods are set as $n = 100$, $m = 50$ and $s = 50, 100, 150, 200$. The size of networks is set to 1000.

Based on the above mentioned method, we sample the structure solution space and provide the relationship between cooperation level and coverage rate in Figure 9. Obviously, the data are linearly distributed and the correlation between coverage rate and cooperation level of population structures tends to be positive.

So far, we have verified our previous inference that highly cooperative population structures are usually accompanied by larger influence coverage rate. However, just a high influence coverage rate may not guarantee

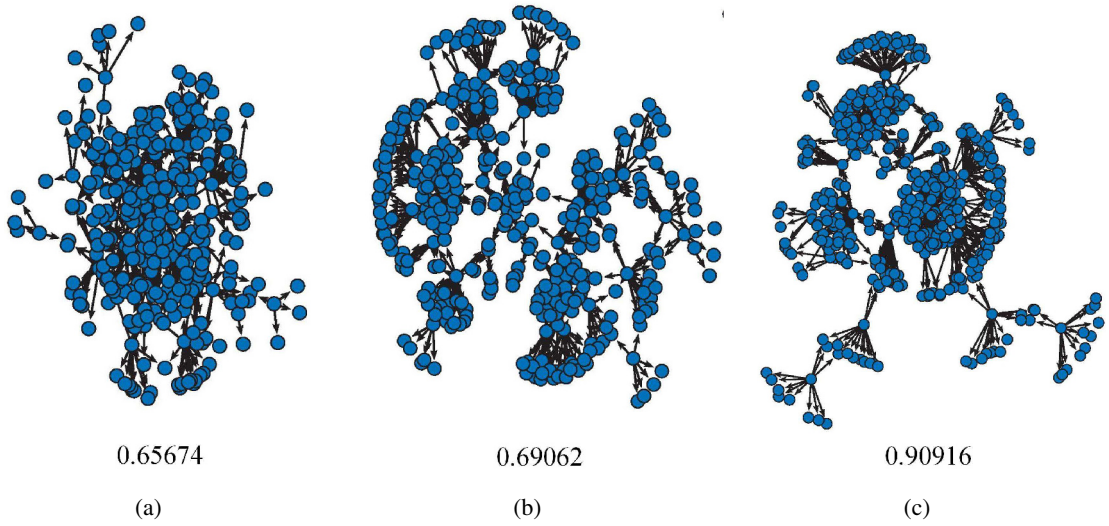

Fig. 6. Influence transmission structures of BAN (a), HKN: $p = 1$ (b), mlSFNs (c) when the size of networks is 500, $m_0 = 2$, and average connection $z = 4$. We ignore the isolated and almost isolated (very few) nodes in the above figures. And corresponding average influence coverage rate (when $r = 1$) of different network models is provided below the graphs, respectively. These influence coverage rate are obtained through averaging over 100 independent runs. Obviously, mlSFNs have the largest average coverage rate while HKNs follows.

Algorithm 2: Sampling methods

Input:
n: number of samplings;
s: adjustment scale;
m: search pace;

Output:
D: data set of the samplings containing corresponding coverage rate and cooperation level;

1: **for** $i = 1$ to n **do**
2: Randomly select a scale-free network model from BANs, HKNs and mlSFNs;
3: Generate a network G and its copy G' based on the selected model;
4: **for** $j = 1$ to m **do**
//Corresponding iteration of edge adjustment is s.
5: Employ the edge switch method to adjust G and increase the corresponding coverage rate;
6: Employ the edge switch method to adjust G' and decrease the corresponding coverage rate;
//Evaluation of cooperation level is obtained through averaging over 100 independent runs.
7: Evaluate the influence coverage rate and cooperation level of G and G';
// save influence coverage rate of structures pairs with corresponding cooperation level
8: Save the relational data to D if data is new;
9: **end;**
10:**end;**

a highly cooperative structure. Apparently, if the top node (n) in Figure 3 is initialized as a defector, it is necessary that node n (unaffected nodes) should be as less influential as possible. In this case, we further complement the rule that may be shared by cooperative structures and formulated it by (5). f_1 is to calculate the influence coverage rate of a given structure G and f_2 is to calculate the influence strength of the unaffected nodes. To be mentioned, f_2 should be designed subject to different strategy update rules due to different influence strength, respectively. Design and calculation approach of f_2 will be provided in the following experiment part:

$$E = f_1(G) - f_2(G). \tag{5}$$

Given equation (5), a fast structure optimization algorithm that employs the above empirical formula as prior experience is proposed. This algorithm is termed as fMA-C_{PD}-SFN and is designed to optimize an input population structure without changing its original degree distribution, which is in consideration of the heterogeneity of individuals in reality. For example, different predation capability leads to different interaction with other individuals in the population.

Although an approach has been proposed in [40] to optimize population structure, many problems still remains to be solved: (1) The computational cost of the algorithm proposed in [40] is too high, which is unacceptable to provide real-time optimization or to solve large-scale

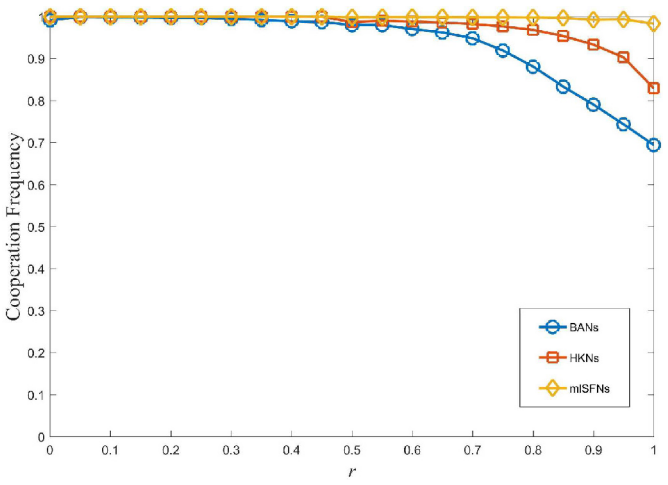

Fig. 7. Cooperation frequency of different scale-free network models (5000 nodes, $m_0 = 2, z = 4$) under different r. The corresponding result shown above are obtained by averaging over 300 independent runs (evaluation times: 30 (independent evaluations) $\times$ 10 (different networks) = 300). Apparently, the cooperation level of mlSFNs is the highest while that of HKNs ($p = 1$) follows. Each equilibrium cooperation frequency is calculated through averaging over 1000 generations after a transient period of 100,000 generations

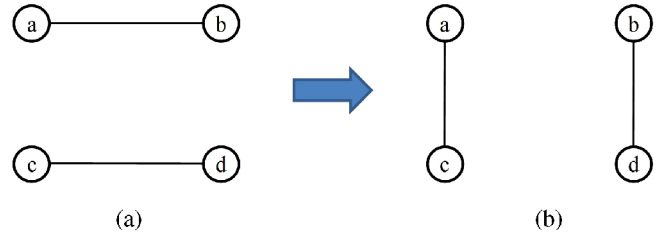

Fig. 8. Illustration of the edge switch method. (a) Initial connection. (b) Connection after adjustment. Two pairs of edges (ab and cd) are randomly selected from the graph. If the targeted created edges (ac and bd) already exist in the graph, another pair of edges will be selected from the graph.

optimization problems, (2) recording large numbers of structure solutions wastes too much storage resource, and (3) operation in reference [40] is too complex and hard to implement. The reason causing these problems is the lack of general rules for optimizing population structure and evaluation variance of cooperation level between runs.

Apparently, calculating E in (5) is much easier than evaluating the cooperation frequency of a structure, thereby saving the computational cost. Meanwhile, the success of fMA-C_{PD}-SFN in optimizing structures subject to different strategy update rules with a higher performance will verify the generality of our rules: influence coverage rate is essential to cooperation while the unaffected nodes should be less influential.

We employ the same basic evolutionary algorithm as in reference [40]. Instead, the local search operation is designed to optimize E of structures rather than cooperation level. Meanwhile, we reserve the statistic average method to approximate the true cooperation level of structures and reduce evaluation error [40].

5 Experiments

We provide a rule that may be shared by cooperative structures based on the previous analysis. And in this section, we apply fMA-C_{PD}-SFN to optimize structures of different populations (BANs and HKNs) subject to different sizes and different strategy update rules. The performance of fMA-C_{PD}-SFN in optimizing a given structure will verify the generality of our rule. Since the local search operator in evolutionary algorithm optimize the E rather than cooperation level, the positive or negative correlation between E and structure's cooperation level will directly influence the final optimization results.

In the first part, we investigate the performance of fMA-C_{PD}-SFN. In the second part, we employ fMA-C_{PD}-SFN with the attempt to optimize large-scale structures. In fMA-C_{PD}-SFN, corresponding parameters are set as $GS = 20$, $Pc = 0.2$, $Sm = 20$, $Sa = 200$, $gen_{max} = 50$, and $TN = 5$. Corresponding parameter of PDG is set to the extreme adverse situation for cooperation: $r = 1$. To avoid unnecessary computational cost, equilibrium cooperation level is calculated through averaging over 0.1 N generations after a transient period of N generations, where N is the size of population structures. Equilibrium of results has been verified in reference [40] and we do not further provide similar analysis in this article.

5.1 Performance of fMA-C_{PD}-SFN on different small-scale structures

In this section, we try to verify the efficiency and adaptability of our rule in advancing the optimization process toward different structures (BANs and HKNs) subject to different strategy update rules (proportional imitation, Fermi rule, and unconditional imitation rule). Apart from the proportional imitation introduced in Section 2, the definitions of Fermi rule and unconditional imitation rule are given as follows:

1. *Fermi rule:* A neighbor (supposed as y) of x is chosen randomly. The probability for y to spring off at site x is $W_{s_x \leftarrow s_y} = 1/(1+\exp(-(P_y - P_x)/k))$, where P_i is the payoff of individual i and $k = 0.1$ is the amplitude of noise.
2. *Unconditional imitation rule:* Each individual x imitate the strategy of its neighbor y with the largest payoff, provided $P_y > P_x$.

In the previous section, we provided equation (5) to formulate our rule: f_1 calculates the percent of nodes x with a neighbor y satisfying $P_y \geq P_x \propto d_y \geq \alpha d_x$ in the first generation. Specific α can be approached by solving inequality $P_y \geq P_x$ based on the parameters of the game and is irrelevant to the strategy update rules. However, the second part (f_2) of unaffected nodes' influence strength should be designed according to different strategy update rules (suppose these nodes are imaginary defectors):

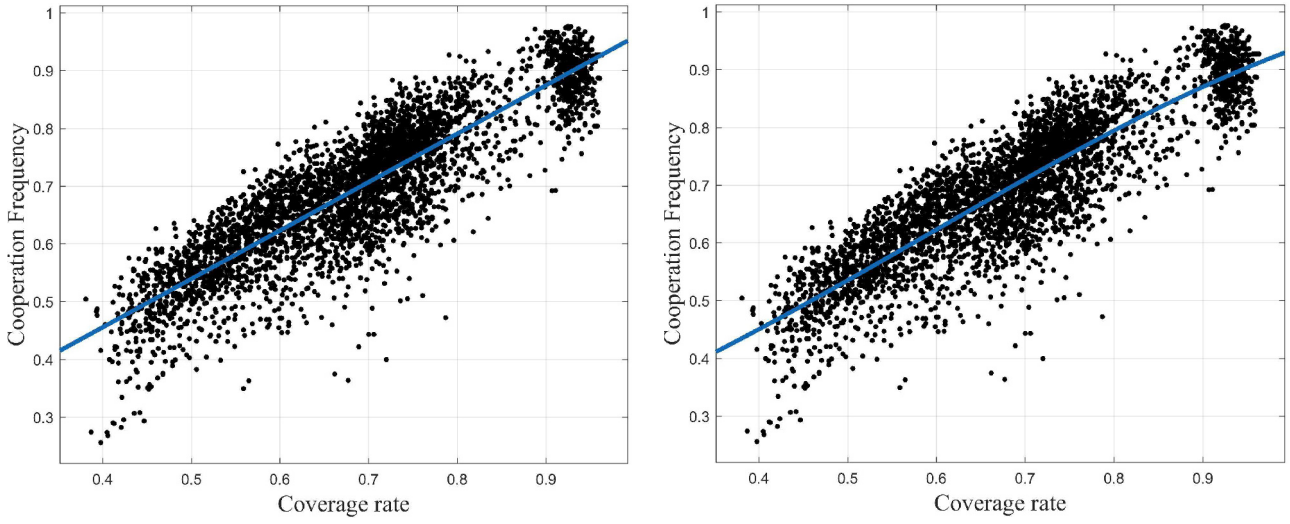

Fig. 9. Relationship between coverage rate and cooperation level. Different functions are employed to fit the sampling data: (a) Polynomial function. (b) Gaussian function. Apparently, fitting curve exhibits good linearity subject to different fitting functions. Therefore, we can conclude that the coverage rate and cooperation level of population structure have a strong positive relationship, and tend to be linearly related. Each equilibrium cooperation frequency is calculated through averaging over 200 generations after a transient period of 2000 generations. Equilibrium of results under this simulation time can be referred from reference [40].

Algorithm 3: Fast structure optimization algorithm to optimize scale-free structures for the promotion of cooperation in the Prisoner's dilemma game (fMA-C$_{\mathrm{PD}}$-SFN)

Input:
G_0: Initial scale-free network;
GS: Size of EA population;
Pc: Crossover rate;
Sm: Mutation scale;
Sa: Adjustment scale;
gen_{max}: Maximum number of iterations;
TN: Test number of evaluations;
Output:
G^*: Optimized structure;

1: Adjusting $G_{i-1}(i \leq GS)$ based on the edge switch method (scale: S_a) to produce G_i and initialize EA population;
2: Evaluate the cooperation level of EA population through averaging over TN independent runs;
3: The roulette selection is employed to select parents and EA population reproduce with crossover rate P_c;
4: Offspring structure solution mutate on the edge switch method (scale: S_m);
5: Evaluate the cooperation level of the offspring solutions through averaging over TN independent runs;
6: Calculate E (cooperation estimation) of both parents and offspring;
7: Conduct the local search (details see Algorithm 4) upon both the parents and the offspring (scale S_a);
8: If the iteration generation exceeds gen_{max}, output the current best population structure; otherwise, the best GS solutions in terms of cooperation level are selected as parents for the next generation and go to 3.

1. *Proportional imitation and Fermi rule:* f_2 calculates the average probability that an unaffected node may transfer defection to its neighbors in the first generation.
2. *Unconditional imitation rule:* f_2 calculates the largest expected payoff difference between the unaffected node x and its neighbor y in the first generation. $f_2(G) = 1/(1 + \exp(-(P_x - P_y)/k))$.

Three different experiments have been conducted to verify that our rule has provided effectively positive guidance to the optimization process. As can be seen in Figure 10, fMA-C$_{\mathrm{PD}}$-SFN successfully optimizes different structures subject to different strategy update rules and the output structures have high cooperation level. Our preceding research reveals that small population structures are usually accompanied by larger evaluation variance [40], which leads to a commonly accepted problem that fails the optimization process of evolutionary algorithm (EA cheat). To deal with this problem, mlEA-CPD-SFN [40] has introduced lots of additional components, which sacrifice storage space and are computational expensive. Meanwhile,

Algorithm 4: Local search

Input:
P: Parent population and offspring population;
C: Cooperation level of structures;
E: Cooperation estimation of structures;
TN: Test number of evaluations;
Output:
G^*: Optimized structure;

for every structure G_i in P **do**
  Conduct the edge switch method upon G_i to optimize its E based on the hill climbing method;
  Evaluate the cooperation level of the adjusted structure G_i' through averaging over TN runs;
  if(C_{Gi}>C_{G_i}') //original structure has higher cooperation level
    Another TN runs of evaluations upon G_i are conducted;
    //Corresponding sum of evaluation results and number of evaluation runs are updated.
    Update the cooperation level of G_i through combining results of the new TN runs;
    Abandon G_i' and keep G_i in the population;
  else
    Replace G_i with G_i';
  end;
end;

Table 1. The number of evaluations and running time of fMA-C_{PD}-SFN and mlEA-CPD-SFN when optimizing the same population structure under $r = 1$. OpenMP skill is employed to accelerate the local search part of these algorithms.

1000 BANs	mlEA-CPD-SFN$_5$	fMA-C_{PD}-SFN
Cooperation level (after optimized)	0.79991	0.9437
Running time	15587.8s	1811.45s
Evaluation number	128064	19645
500 BANs	mlEA-CPD-SFN$_5$	fMA-C_{PD}-SFN
Cooperation level (after optimized)	0.6848	0.8172
Running time	3293.25s	392.76
Evaluation number	114853	21140

simulation results in Table 1 have reflected that the efficiency of fMA-C_{PD}-SFN is much higher than those of mlEA-CPD-SFN (details in Ref. [40]), thus fMA-C_{PD}-SFN has an obviously better performance. Most importantly, we change the local search target in fMA-C_{PD}-SFN from E to clustering coefficient and find corresponding algorithm (fEAcluster) to fails in optimization (Fig. 11). All these phenomena verify that our rule formulated by E actually has a positive correlation with cooperation subject to different strategy update rules and network sizes. Even if this rule is inspired from the analysis of game dynamics under the proportional imitation, the essence of our rule is the probability of strategy spread.

5.2 Performance of fMA-C_{PD}-SFN on large-scale structures

In the previous sections, we verified the positive correlation between our rule and cooperative structures. Since employing this rule as a prior experience can effectively guide the optimization process and reduce the computation complexity, we further analyze the efficiency of fMA-C_{PD}-SFN in optimizing larger scale structures. In contrast, mlEA-CPD-SFN cannot support the optimization toward larger scale structures due to its high computational complexity. Considering the simulation time, we only provide results obtained under the proportional imitation. Obviously, evolutionary algorithm (fMA-C_{PD}-SFN) successfully optimizes population structures with 5000 nodes and promotes the cooperation in PDG (Fig. 12). Even if E effectively decreases the computational cost required during the optimization, a faster method to deal with large-scale structures and evaluate the cooperation level of structures remains to be a bottleneck to a real-time optimization algorithm.

6 Conclusions

How to control and regulate strategy distribution within a network system has attracted lots of attention. With the rapid development of technology, the demand to improve the cooperation level of a large-scale network system results in a new challenge. Meanwhile, a highly cooperative group as a result of species evolution has been found significant to the promotion of a group's competitiveness and intrinsically efficiency. Thus, learning from the organization of the cooperative network system composed by self-interested agents and reveal control methods for the promotion of cooperation should be a significant task.

In this article, we attempt to provide a more general rule to help control the cooperation level of a network system

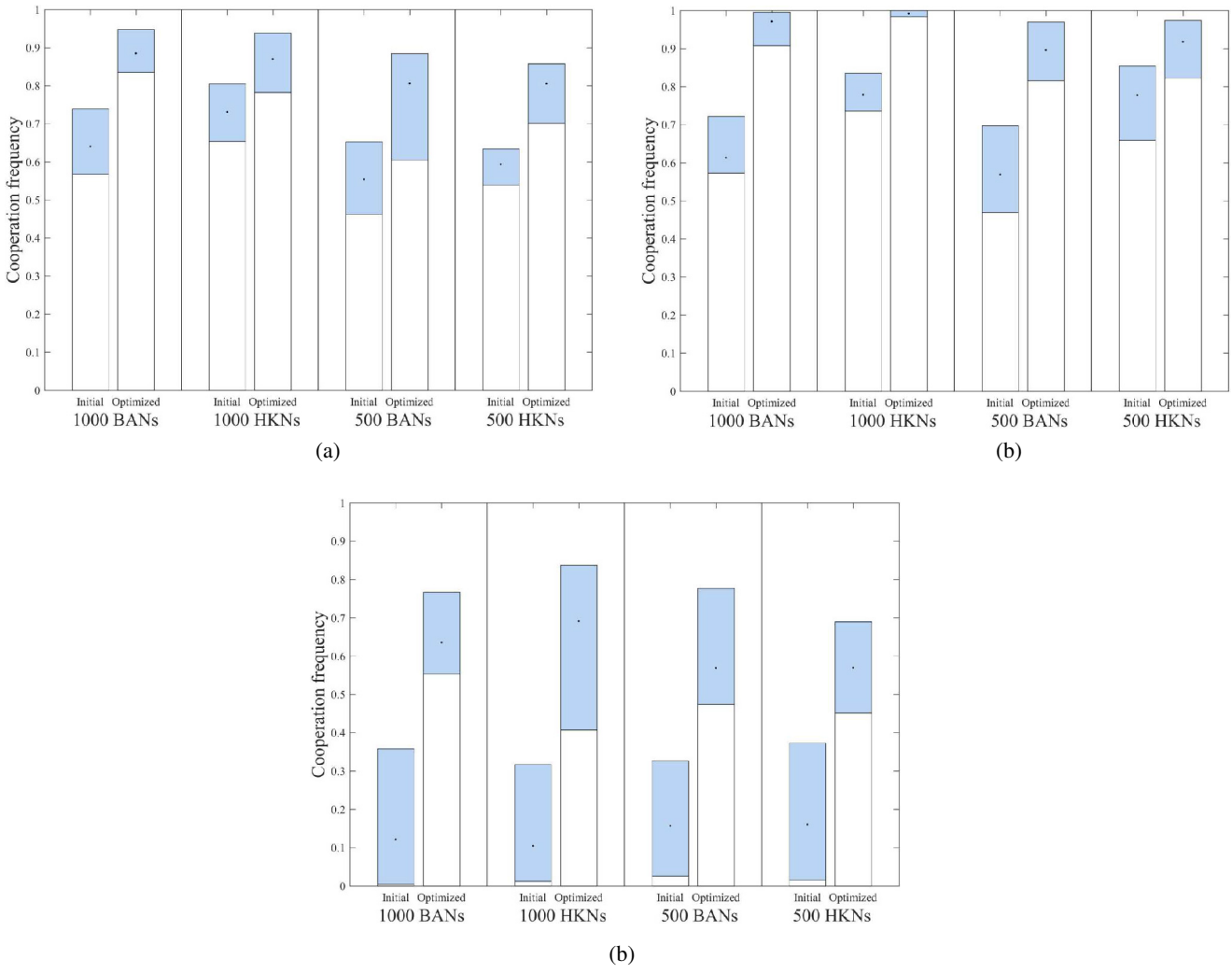

Fig. 10. Optimization results of fMA-C_{PD}-SFN subject to different network sizes and strategy update rules. Three different strategy update rules are considered in the experiments: (a) proportional imitation, (b) Fermi rule, and (c) unconditional imitation rule. In each subfigure, we provide optimization results of four types of structures, respectively, given in four regions: BANs (1000 nodes), HKNs (1000 nodes), BANs (500 nodes), and HKNs (500 nodes). In each region, we provide the cooperation level of 10 independent structures before and after the optimization, with black points marking the corresponding mean values. Cooperation level of each structure has been repeatedly evaluated 500 times to reduce the variance. For example, the left region in part (a) provides the initial and optimized cooperation level of 10 BANs with 1000 nodes. Cooperation distribution of each structure group lays within the blue bar. As can be seen, structures optimized by fMA-C_{PD}-SFN have obviously higher cooperation level than the initial BANs with 1000 nodes. Overall, fMA-C_{PD}-SFN successfully optimizes the population structures and promotes cooperation subject to different network sizes and strategy update rules.

playing the prisoner's dilemma game. Analysis of game dynamics from micro perspective leads to the discovery of correlation between cooperation and influence structure. Besides, the high cooperation level of multilevel scale-free networks (mlSFNs) and simulation results of relational analysis support our preliminary inference: influence coverage rate is essential to cooperation while the unaffected nodes should be less influential. To verify that this rule may be shared by cooperative structures subject to different strategy update rules, we introduce this rule to guide the optimization process of evolutionary algorithm. Our results reflect that this rule provides an efficient positive guidance to the optimization process subject to different network sizes and strategy update rules, which verify the generality and effect of our rule in optimizing cooperation level of structures. Thus, we conclude that this rule is instructive for future design of a highly cooperative population structure.

This work was supported in part by the Outstanding Young Scholar Program of National Natural Science Foundation of China (NSFC) under Grant 61522311, in part by the General Program of NSFC under Grant 61773300, and in part by the Key Program of Fundamental Research Project of Natural Science of Shaanxi Province, China under Grant 2017JZ017.

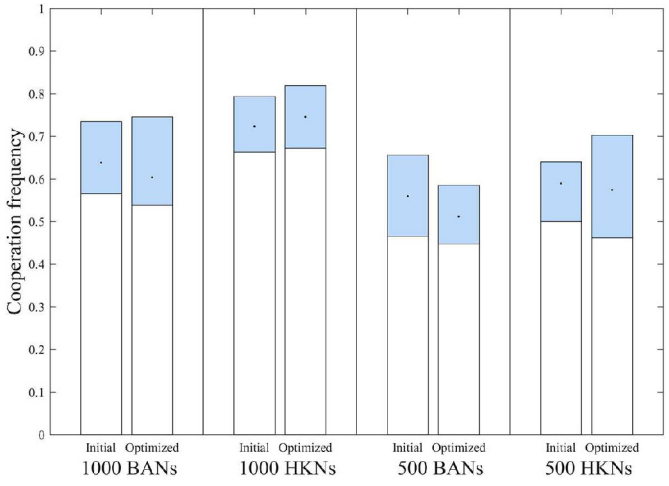

Fig. 11. Optimization results of fEAcluster subject to different network sizes under proportional imitation. We provide optimization results of four types of structures, respectively, given in four regions: BANs (1000 nodes), HKNs (1000 nodes), BANs (500 nodes), and HKNs (500 nodes). In each region, we provide the cooperation level of 10 independent structures before and after the optimization (blue bar), with black points marking the corresponding mean values. Cooperation level of each structure has been repeatedly evaluated 500 times to reduce the variance. Apparently, $\text{fEA}_{\text{cluster}}$ fails to optimize the population structures and promote cooperation.

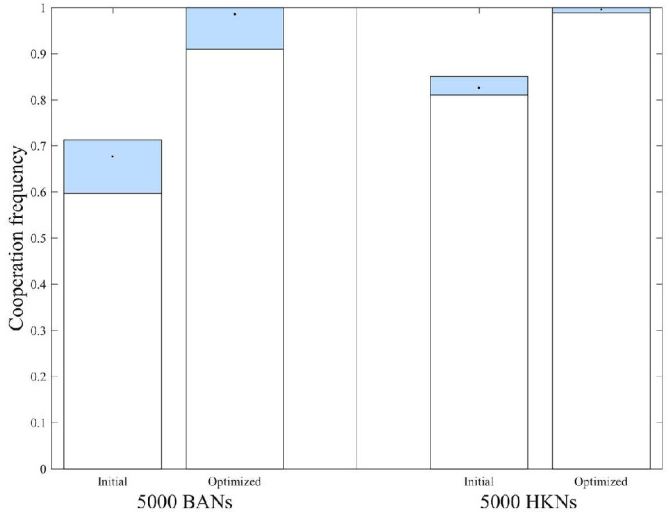

Fig. 12. Optimization results of fMA-C_{PD}-SFN to structures with 5000 nodes under proportional imitation. We provide optimization results of two types of structures, respectively given in two regions: BANs (5000 nodes) and HKNs (5000 nodes). In each region, we provide the cooperation level of 10 independent structures before and after the optimization (blue bar), with black points marking the corresponding mean values. Each structure has been repeatedly evaluated 500 times to reduce the variance. Apparently, fMA-C_{PD}-SFN successfully optimizes those large-scale population structures and promotes the cooperation.

Author contributions statement

Penghui Liu and Jing Liu devised the research project; Penghui Liu performed numerical simulations and analyzed the results; Penghui Liu and Jing Liu wrote the article.

References

1. P. Peng, Y. Wen, Y. Yang, Q. Yuan, Z. Tang, H. Long, J. Wang, arXiv:1703.10069 (2017)
2. M.A. Nowak, R.M. May, Nature **359**, 826 (1992)
3. R. Chiong, M. Kirley, IEEE Trans. Evol. Comput. **16**, 537 (2012)
4. J. Li, G. Kendall, IEEE Trans. Evol. Comput. **18**, 819 (2014)
5. C. Wedekind, M. Milinski, Science **288**, 850 (2000)
6. E. Fehr, U. Fischbacher, Nature **425**, 785 (2003)
7. M.A. Nowak, K. Sigmund, Nature **437**, 1291 (2005)
8. M.A. Nowak, Science **314**, 1560 (2006)
9. X. Chen, F. Fu, L. Wang, Physica A **378**, 512 (2007)
10. Y. Li, J. Zhang, M. Perc, Appl. Math. Comput. **320**, 437 (2018)
11. A. Szolnoki, M. Perc, New J. Phys. **20**, 013031 (2018)
12. E. Lieberman, C. Hauert, M.A. Nowak, Nature **433**, 312 (2005)
13. H. Ohtsuki, C. Hauert, E. Lieberman, M.A. Nowak, Nature **441**, 502 (2006)
14. B. Allen, M.A. Nowak, EMS Surv. Math. Sci. **1**, 113 (2014)
15. F.C. Santos, J.F. Rodrigues, J.M. Pacheco, Proc. R. Soc. Lond B **273**, 51 (2006)
16. C. Hauert, M. Doebeli, Nature **428**, 643 (2004)
17. F.C. Santos, J.M. Pacheco, Phys. Rev. Lett. **95**, 098104 (2005)
18. M. Perc, A. Szolnoki, Phys. Rev. E **77**, 011904 (2008)
19. F.C. Santos, M.D. Santos, J.M. Pacheco, Nature **454**, 213 (2008)
20. A. Szolnoki, M. Perc, Z. Danku, Physica A **387**, 2075 (2008)
21. L. Luthi, E. Pestelacci, M. Tomassini, Physica A **387**, 955 (2008)
22. A. Szolnoki, M. Perc, EPL **113**, 58004 (2016)
23. A. Szolnoki, M. Perc, Sci. Rep. **6**, 23633 (2016)
24. M. Perc, A. Szolnoki, G. Szabó, Phys. Rev. E **78**, 066101 (2008)
25. Z. Wang, A. Szolnoki, M. Perc, EPL **97**, 48001 (2012)
26. Z. Wang, L. Wang, A. Szolnoki, M. Perc, Eur. Phys. J. B **88**, 124 (2015)
27. D.Y. Kenett, M. Perc, S. Boccaletti, Chaos Solitons Fractals **80**, 1 (2015)
28. Z. Wang, A. Szolnoki, M. Perc, Sci. Rep. **3**, 2470 (2013)
29. S. György, F. Gábor, Phys. Rep. **446**, 97 (2007)
30. C. Xia, X. Li, Z. Wang, M. Perc, New J. Phys. **20**, 075005 (2018)
31. M.G. Zimmermann, V.M. Eguíluz, M.S. Miguel, *Economics with Heterogeneous Interacting Agents*, Lecture Notes in Economics and Mathematical Systems (Springer, Berlin, 2001)
32. A. Szolnoki, M. Perc, EPL **86**, 30007 (2009)
33. A. Szolnoki, M. Perc, New J. Phys. **11**, 093033 (2009)
34. A. Szolnoki, M. Perc, Z. Danku, Europhys. Lett. **84**, 88 (2008)

35. J.M. Pacheco, A. Traulsen, M.A. Nowak, J. Theor. Biol. **243**, 437 (2006)
36. J.M. Pacheco, A. Traulsen, M.A. Nowak, Phys. Rev. Lett. **97**, 258103 (2006)
37. M. Perc, A. Szolnoki, Biosystems **99**, 109 (2010)
38. C. Shen, C. Chu, L. Shi, M. Perc, Z. Wang, R. Soc. Open Sci. **5**, 180199 (2018)
39. B. Allen, G. Lippner, Y. Chen, B. Fotouhi, M.A. Nowak, S. Yau, Nature **544**, 227 (2017)
40. P. Liu, J. Liu, Sci. Rep. **7**, 4320 (2017)
41. M. Zhou, J. Liu, IEEE Trans. Cybern. **47**, 539 (2014)
42. Y. Chi, J. Liu, IEEE Trans. Fuzzy Syst. **24**, 71 (2016)
43. W. Zhong, J. Liu, M. Xue, L. Jiao, IEEE Trans. Syst. Man Cybern. B **34**, 1128 (2004)
44. C. Liu, J. Liu, Z. Jiang, IEEE Trans. Cybern. **44**, 2274 (2014)
45. M. Zhou, J. Liu, Physica A **410**, 131 (2014)
46. Y. Yuan, H. Xu, B. Wang, B. Zhang, X. Yao, IEEE Trans. Evol. Comput. **20**, 180 (2016)
47. X. Qiu, J.X. Xu, K.C. Tan, H.A. Abbass, IEEE Trans. Evol. Comput. **20**, 232 (2016)
48. J. He, G. Lin, IEEE Trans. Evol. Comput. **20**, 316 (2015)
49. W. Du, W. Ying, G. Yan, Y. Zhu, X. Cao, IEEE Trans. Circuits Syst. II Express Briefs **64**, 467 (2017)
50. W. Du, Y. Gao, C. Liu, Z. Zheng, Z. Wang, Appl. Math. Comput. **268**, 832 (2015)
51. S. Assenza, J. Gómez-Gardeñes, V. Latora, Phys. Rev. E **78**, 017101 (2008)
52. A. Yamauchi, J. Tanimoto, A. Hagishima, BioSystems **102**, 82 (2010)
53. A.L. Barabàsi, R. Albert, Science **286**, 509 (1999)